

The Tesys Rail Project: Innovative Models to Enhance the Energy Sustainability of Railway Systems

A. Frilli¹, E. Meli¹, D. Nocciolini¹, L. Pugi¹, A. Rindi¹, B. Romani¹
M. Ceraolo², and G. Lutzemberger²

¹Department of Industrial Engineering, University of Florence, Florence, Italy

²Department of Energy, Systems, Territory and Construction Engineering
University of Pisa, Pisa, Italy

Abstract

Attention to the energy efficiency of railway systems is ever increasing. The research presented in this paper, based on the activities of the TESYS Rail Project, deals with the optimization of railway energy consumptions to increase the efficiency of the system, considering the use of energy storage devices in different operating scenarios, and involving different train typologies. For this purpose, the authors developed an integrated design, simulation and optimization tool, useful also in real time applications. The approach proposed in this paper (based on the analysis of the interactions between the vehicle longitudinal dynamics and the electrical line), characterized by a high numerical efficiency, has been experimentally validated considering as a test case the Italian high speed train ETR 1000 and used to investigate the feasibility of energy storage devices in High Speed railway systems.

Keywords: railway energetic optimization, longitudinal dynamics, regenerative braking, contact line, electrical substations, energy storage, line-vehicle interactions.

1 Introduction

According to the data available in the literature [1], more than 30% of the total CO₂ emission of the European community is still caused by transport systems (see Figure 1). Currently the impact of railway systems, in terms of ratio between equivalent emissions and transported load (usually expressed in gCO₂/pkm), is less than one third with respect to the other ground and air concurrent systems [2, 3]. As a consequence, the sustainability of railway systems is widely recognized. However, as reported in Figure 2, it is a common opinion that the technology trend will produce a significant improvement of the efficiency of cars and planes, with an estimated reduction of the

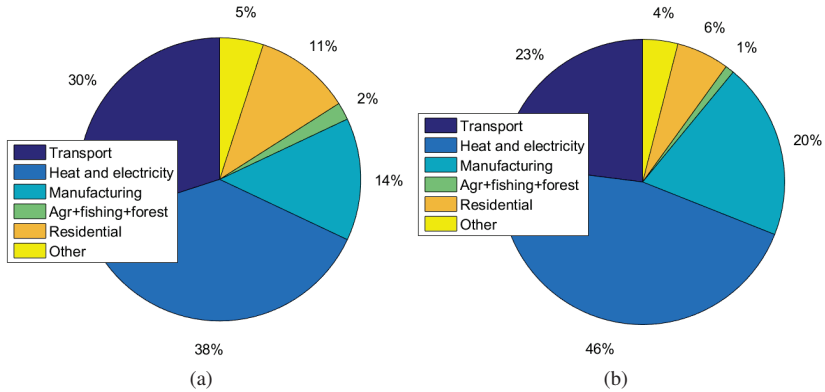


Figure 1: CO₂ sources: (a) Europe, (b) world.

CO₂ emissions of more than the 50% by the year 2050, thus strongly reducing the leadership of railway in terms of sustainability. Railways will face the challenge of more efficient competitors and, consequently, they will have to undertake a significant improvement of the efficiency and sustainability of the whole system, in order to meet the challenges of the future [4]. It is important to underline, in order to avoid misunderstandings and to clarify the meaning of the whole paper, that the sustainability mentioned in this paper should be a reduction of the environmental impact of railway transportation by improving the global efficiency of the systems devoted to the control of train longitudinal dynamics.

Furthermore, the railway system has already undergone a critical phase of change for the energy billing and management: the free energy market and the need for the vehicle to be interoperable between different energy infrastructures, managements and suppliers, considering also the presence of multiple carriers and railway operator have made it mandatory to be able to correctly calculate and measure the vehicle energy consumption and the losses due to the various elements of the vehicle-line system. An example of a system, where different multiple stakeholders interact within a railway system, is shown in Figure 3.

The purpose of the Tesys Rail Project (acronym of “Methods and Instruments to improve environmental sustainability of railway systems”) is to increase the sustainability of railway systems by combining the know-how of eight major research and industrial partners, such as Ansaldo STS, Thales, ATS PMI Toscana, Fondazione Politecnico di Milano, University of Florence and the University of Naples. In particular this work deal with the activities coordinated by University of Florence, concerning the optimization of energy consumptions through the use of energy storage systems, in order to increase the efficiency of the whole system, recovering braking energy, reducing power losses and avoiding problems due power peaks on the line.

Figure 4 shows the scenarios considered for the development of the proposed ap-

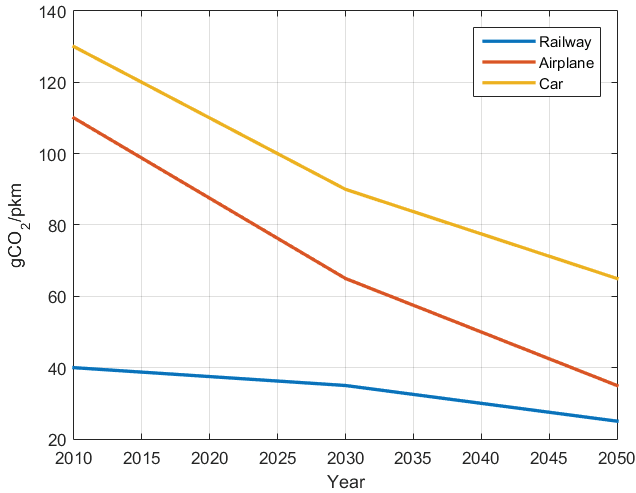


Figure 2: Comparison between the CO₂ emissions of different transport methods.

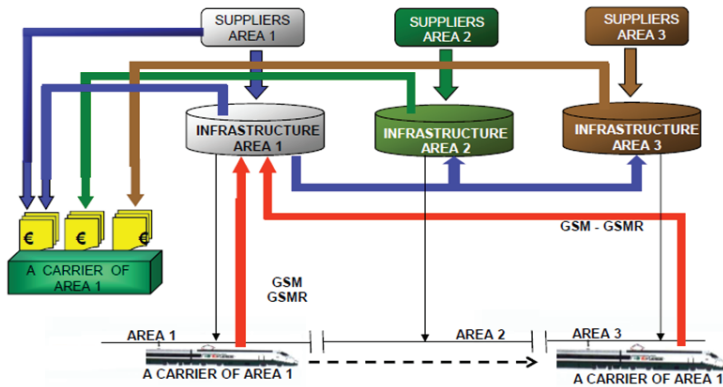


Figure 3: Energy billing and management.

proach: from a standard case without energy recovery, it is possible to intervene by adding stationary energy storage devices.

Regenerative braking represents one of the greatest sources of savings for modern trains with distributed traction systems. The use of regenerative braking allows significant energy savings and to avoid the use of classical dissipative brakes (both electrical and pneumatic), thus providing also important advantages in terms of maintenance costs, wear and pollution [5–7].

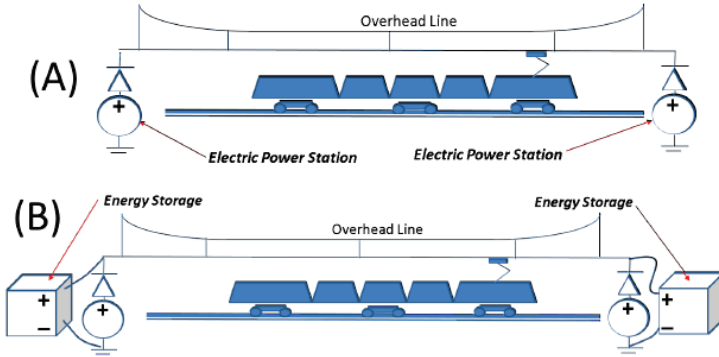


Figure 4: Energy storage scenarios.

The recovery of the train kinetic energy, during the braking phases requires the presence of a load or a storage system, which can handle the energy fluxes [8, 9]. The maximum power, produced by the train during the braking phase, is roughly proportional to train mass, speed and deceleration:

$$W_{r,max} \propto m_i \dot{x}_{max} \ddot{x}_b \quad (1)$$

where \dot{x}_{max} is the maximum train speed before the deceleration, \ddot{x}_b is the imposed deceleration and m_i is the train inertia. A full list of the nomenclature used in this paper is found at the end of the paper.

Furthermore, the mean recovered braking power $W_{r,mean}$ is proportional to the vehicle kinetic energy and to the braking occurrence f_b (i.e. the number of braking phases with respect to traveling time):

$$W_{r,mean} \propto m_i \dot{x}_{max}^2 f_b \quad (2)$$

The mean recovered power $W_{r,mean}$ in tramways applications is relatively high with respect to the power peak value; this is due to the smaller inertia and speeds and to the higher braking frequency. This scenario is particularly favorable for the use of regenerative braking systems and, since the lines are usually shorter than conventional railway lines, it is also possible to easily implement innovative customized solutions. For these reasons, the application of energy recovery systems in tramways and light railways has been widely analyzed [10–12], considering various energy storage systems locations [13, 14], different applications and usage [15–18], and different storage technologies [19]. Energy recovery in high speed railway systems is still an open field of research and the possibility to obtain significant savings is remarkable.

This research work starts from a consolidated know-how [13, 20] on the energy optimization of tramways and the simulation of railway systems. The first purpose of the

activity is to investigate how the usage of energy storage to recover energy can really improve efficiency in different complex operating scenarios, also involving different train typologies, such as high speed trains or more conventional railcars used for regional or urban transports. A second objective of the activity is the development of integrated design, simulation and optimization tools able to be easily shared from a restricted group of researchers to a wider community of research and industrial partners. The final objective of the activity is the generation of a model that can be integrated in real time applications, reaching a good compromise between the accuracy of the results and numerical efficiency of the approach.

The core of the proposed model is based on the development of a computationally efficient model of the railway vehicle longitudinal dynamics (see Figure 5); this model is devoted to the optimization of the system and of its mission profiles in terms of efficiency, sustainability and reliability. In particular, the model is able to reproduce the following phenomena:

- Longitudinal dynamics of the train: the mechanical behavior of the system is a result of the interactions between traction and braking forces and resistances to motion (both due to the vehicle and line induced and including the limitations that arise from limited wheel-rail adhesion);
- Power demand and energy flows: energy consumption and recovery, efficiency, calculated currents and corresponding interactions with the surrounding infrastructure, energy management;
- Electrical behaviour of contact line and electrical substations, including stationary energy storage devices.

The model has been developed in order to obtain the following characteristics:

- General and scalable approach: the model is able to reproduce a variety of different scenarios, ranging from light railway and tramway systems to freight and passenger trains (including high speed trains);
- Modularity: the model is easily adaptable to different system configurations, allowing the analysis of different energy saving techniques;
- High level language: the use of a high level modeling environment allows an easier maintenance and usage for industrial and research applications;
- RT Implementation: the model provides a good compromise between accuracy and numerical efficiency and can be used to produce tool for real time applications like diagnostic, monitoring or control applications;
- Portability: the model is easily adaptable to different target/real time environment (different RTOS or even micro-controllers).

The development of efficient numerical models for the simulation and for the optimization of railway vehicle systems is an open research field and has a great industrial interest, as stated by recent contributions available in literature [20]. Most of these works [9, 13, 15–17], deal with the application of energy recovery and storage techniques to improve the efficiency of the system, reduce voltage and current fluctuations over the line and more generally improve the sustainability of the whole railway system. Most of the techniques used for energy recovery are commonly applied to tramways and light railway applications. In order to extend these techniques to conventional railways, it is necessary to take into account in the train longitudinal dynamics analysis the variability of technical solution that can be adopted for the construction and the control of both traction and braking systems. Such variability is heavily influenced by the type of railway application (freight, conventional passenger or high speed trains). Furthermore, this type of analysis requires an accurate modeling of the braking phase and in particular of the blending between pneumatic braking, electric braking and adhesion independent device such as magnetic track system [21]. Safety and operational issues (such as the distinction between service and emergency braking) also influence the complex interactions between different braking systems [22–24].

This paper is based upon Frilli *et al.* [25], but the current paper includes a more extensive set of experimental data used both to calibrate the model and to perform an experimental validation; furthermore the authors have also analyzed the behaviour of the system with the introduction of a voltage limiter used during regenerative braking, in order to better understand the feasibility of regenerative braking and its impact in high speed systems. The experimental comparisons are referred to the Italian high speed train ETR 1000 and to the Firenze-Roma high speed DC line; in Table 1, the computer characteristics, used to develop and simulate the authors' model, and the model numerical performances have been reported. Concerning the optimization of the whole system, in previous research works, [41], the authors have introduced, within a different model, the concept of automatic optimization of the vehicle mission profile. The research work shown in [41] was more focused on the optimization of the traction system electric parameters; hence, the models proposed in the current research work and in [41] are quite different. In particular, in the cited research work, the authors have suggested the use of the Matlab-Simulink Optimization Toolbox™, which also includes parallel computational features (*i.e.* the possibility of simultaneously simulate multiple models, corresponding to the number of available CPUs on the chosen platform). Parallel computing has been also successfully performed by the authors [42] in order to drastically speed up the execution of complex multibody models. The authors have demonstrated automatic optimization to be feasible and convenient, but it also requires a careful choice of the performance indexes, which have to be numerically robust respect to the input data sets and should be representative of the desired optimum condition, that multi-variable optimization can detect. Consequently, in this research work, the authors have limited their analysis and investigation to manual/iterative methods, in order to better understand and highlight which parameters could have a major impact on the system. In a future work, which is

still in the development phase, the authors will propose a more robust approach to the problem: in fact, within a complex model like that proposed in this research work, automatic numeric optimization is currently feasible but have to be further investigated to reach a higher level of reliability and numerical efficiency.

CPU	Intel CORE i7
Clock frequency	2.30 GHz
RAM memory	8 Gb
Operative system	Windows 10 - 64 bit
$\frac{\text{machine time [s]}}{\text{time to be simulated [s]}}$	$4 \cdot 10^{-4}$

Table 1: Machine features and computational times.

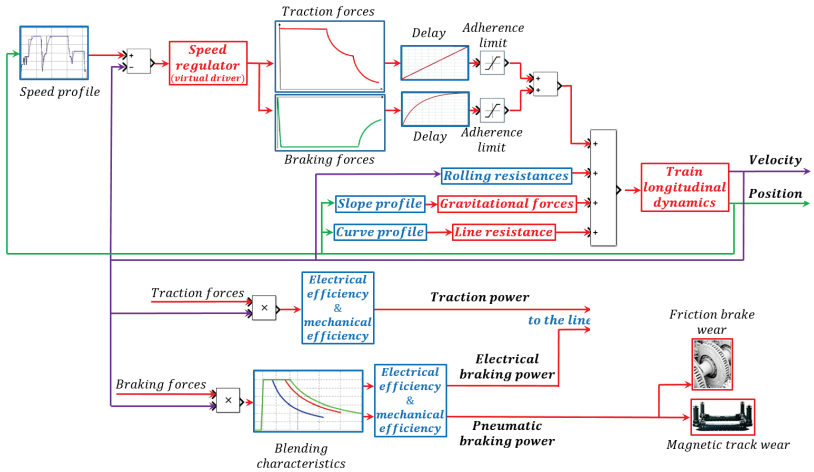


Figure 5: Architecture of the vehicle dynamical model.

2 General architecture of the proposed model

Two schemes of the elements of the proposed model are outlined in Figure 5 and in Figure 6: Figure 5 shows the architecture of the vehicle dynamical model and Figure 6 represents the interactions between the vehicle and the line. A position based speed profile is imposed to the train by a non-linear speed regulator (virtual driver), which controls the application of traction, coasting (no longitudinal effort applied) and braking (service or emergency braking according to the speed error and to the value of the safety state of the train). Traction effort, as in the model used in a previous work [20], is tabulated as a function of speed and line electrification standard, which is an

infrastructure characteristic, dependent on the train position. The traction and braking effort are dynamically applied to the train by using respectively a ramp signal and a delay. Furthermore, the longitudinal efforts are limited by the adherence condition of the line and by the distribution of traction and brake power on each wheelset (*i.e.* by the composition of the train). An innovative feature of the proposed modeling approach is the braking analysis, including the blending of pneumatic and regenerative electric systems: in order to develop a more general modeling tool, a TSI based (acronym of Technical Specifications for Interoperability) approach has been adopted. The TSI are “the specifications by which each subsystem or part of subsystem is covered in order to meet the essential requirements and to ensure the interoperability of the European Community’s high speed and conventional rail systems” [26]. TSI [27–29] and the related EN standards and UIC fiches summarize and impose precise standard to which all the interoperable railway systems has to be constrained. Therefore, a TSI based modeling approach has major advantages in terms of availability of technical data (which are the same that the manufacturer has to produce for the homologation of the vehicle), generality and applicability. Since braking performances are strictly related to the safety of the railway system, the longitudinal braking effort is calculated as a tabulated function of speed, train mass and system state (service braking, emergency braking and optional degraded configurations). Braking performances are not related to the simulation of a specific system configuration (pneumatic or electro-pneumatic braking, magnetic track, electric braking) but to a brake power calculation set by UIC fiches [30,31], EN standards [32] and TSI [26–29]. In order to satisfy these standards, safety specifications not only set limits on the braking performances but also constrain the design of the whole system.

The blending policy and the distribution of braking power between subsystems (electrical and pneumatic) are calculated by a specific sub-component of the vehicle model (as visible in Figure 5) as a function of speed, line state (line voltage and electrification standard) and braking state (service braking, emergency braking, optional degraded configurations). The conversion efficiency is evaluated through tabulated functions: for electrical components, the efficiency depends on current and frequency, while, for mechanical components, it depends on speed and power.

The lumped parameters model of the line, outlined in Figure 6, has been developed using both standard and customized Matlab-Simscape elements. In particular, the line is modeled as a conductor fed by real voltage generators, working in parallel to energy storage devices. The Balance based Bond-Graph approach used to model both vehicle and line elements represents an important innovation with respect to the approach exposed in previous works [20]: authors have abandoned the classical numerical approach of the previous Matlab Simulink implementation, in favour of a Matlab Simscape object oriented modeling [33–35].

Each Simscape block is developed in terms of balance equations and each port represents a bidirectional connection, which transmit variables associated to a physical domain. The new approach is better suited to assure modularity, maintainability and portability on different RTOS targets [36,37].

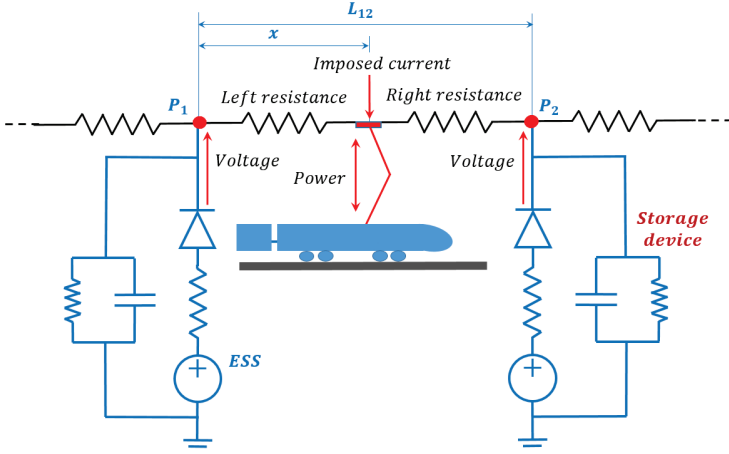


Figure 6: Scheme of the interactions between the vehicle and the line.

For the experimental calibration and validation of the proposed approach, the high speed train ETR 1000 on the direct route Firenze-Roma has been considered (see Figures 7, 11 and 12).

3 Longitudinal dynamics of the vehicle

The mechanical behaviour of the vehicle (*i.e.* its longitudinal dynamics) is simulated according to a quite efficient mono-dimensional model of the train which has been developed in previous research activities and described by:

$$F_t + F_p + F_c + F_a + F_i = 0 \quad (3)$$

where:

- $F_t = \sum F_{t,i}$ is the sum of the longitudinal traction and braking efforts due to the train motorized axles;
- $F_p = -m \cdot g \cdot \sin(\alpha)$ is the gravitational term due to the slope;
- $F_c = -m \cdot g \cdot p_c$ is the lumped contribution due to curves and line design;
- $F_i = -m \cdot \ddot{x}$ is the inertial term and can be used to express the previous equation in order to find the vehicle acceleration;
- $F_a = -m \cdot (a \cdot v^2 + b \cdot v + c)$ is the rolling resistance term.

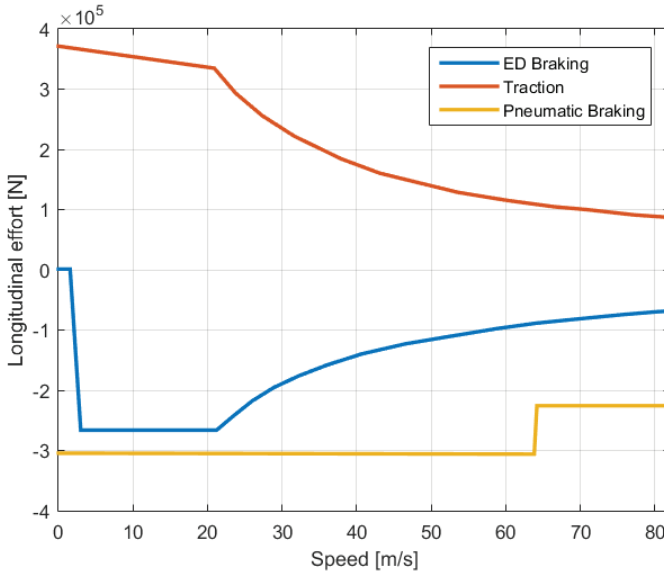


Figure 7: Traction and braking performances of the considered vehicle.

As reported in Figure 7, the traction and braking performances of the vehicle are function of the vehicle speed. In particular, the traction performance is characterized by three different trends:

- A first part where the traction effort is constant;
- A second part where the traction effort trend is hyperbolic and the vehicle power is constant;
- A last part where the vehicle power is inversely proportional to speed.

For trains that can be fed by different electrification standards, it is possible to define more than one traction-braking performance curve. Furthermore, it is useful to define those curves also for degraded adhesion condition; this is especially important for the braking efforts. Figure 8 shows two possible blending strategies for the braking phase: the first case is the blending according to the performance of a TSI compliant pneumatic brake, while the second one is the blending according to tabulated TSI compliant limits.

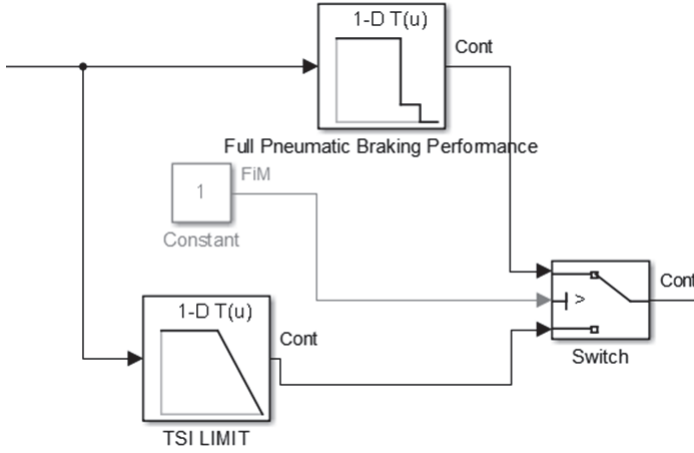


Figure 8: Blending strategy.

4 Line and electrical substations

The electric line model is composed of a simple contact line model fed by electrical substations, distributed throughout the line itself; the line supply the vehicle with the energy needed for its motion and it is also able to receive the energy produced by the vehicle during the regenerative braking phases. The energy due to those phases can be directly supplied to other accelerating vehicles present on the track or stored in energy storage devices, placed corresponding to some substations. During a dynamic simulation, the train position within the line varies and, hence, it modifies the line configuration; in particular, the line resistance between two vehicles or between a vehicle and the electrical substations varies with time (*i.e.* the left and right line resistances observed by the train as reported in Figure 6 are function of the vehicle position).

Those resistances can be calculated according to:

$$\begin{cases} R_{left} = (1 - \delta) \cdot R_{tot} \\ R_{right} = \delta \cdot R_{tot} \\ \delta = \frac{L_{12} - x}{L_{12}} \end{cases} \quad (4)$$

where δ is the ratio between the distance of the train from the next substation ($L_{12} - x$) and the distance between the two substations. These Equations are referred to the case of a bilateral power condition (*i.e.* when the vehicle moves between two substations). Figure 9 shows a scheme of the electrical balance on which the line model is based; in particular, the line node, where the energy is fed to the vehicle, is controlled by the

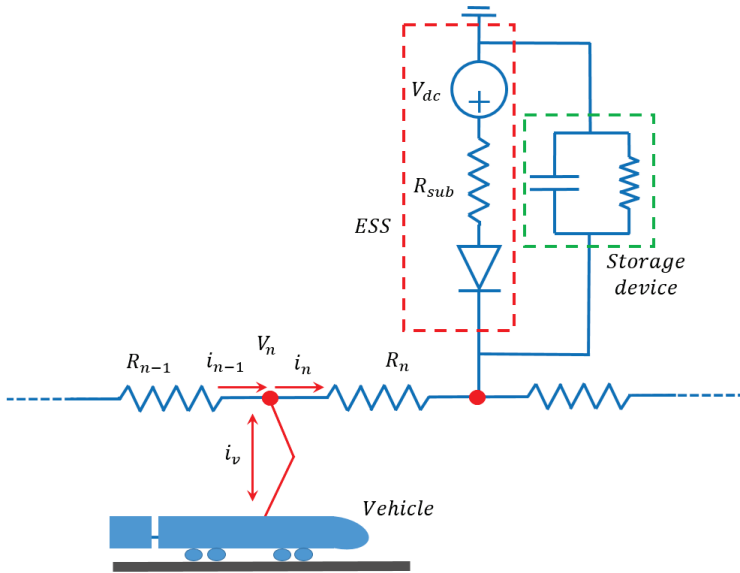


Figure 9: Scheme of the contact line model.

following Equations:

$$\begin{aligned} i_{n-1} - i_n &= i_v + i_c \\ V_{n+1} &= V_n - R_n \cdot i_n \end{aligned} \quad (5)$$

where i_n is the current which leaves the n -th node, V_n is the voltage, i_v is current required or provided by the vehicle and R_n is the resistance of the corresponding line part. The current required by the vehicle during the traction phase (or equivalently, the current provided to the line during the regenerative braking phases) can be calculated from the vehicle power, considering the efficiency of the electrical and mechanical components of the system:

$$W_t = \frac{W_{wheels}}{\eta_{gearbox} \cdot \eta_{motor} \cdot \eta_{motordrive}} \quad (6)$$

$$W_b = W_{wheels} \cdot \eta_{gearbox} \cdot \eta_{motor} \cdot \eta_{motordrive}$$

The electrical substations main function is to feed the line approximating an ideal voltage source. They are often based on passive not reversible devices: a typical substation transform the alternate current provided by the grid into direct current to feed the vehicle. Thus, the substation can be modelled as an ideal voltage source, connected in series with a resistance (to represent the source internal voltage drop) and a diode. Furthermore it is also possible to consider the case of trains directly fed with the alternate current (i.e. like the high speed train considered in this paper for the validation of the model). The substation model can also include a stationary

energy storage device. The node where the substation is connected to the contact line is represented by the following Equations:

$$\begin{aligned} V_{dc} - (i_n - i_{n-1}) \cdot R_{sub} &= V_n \\ V_{n+1} &= V_n - R_n \cdot i_n \end{aligned} \quad (7)$$

where V_{dc} is the voltage provided by the ideal voltage source and R_{sub} is the substation internal resistance.

5 Energy storage systems

Through the proposed model, it is possible to consider the effect on the system of different types of storage devices. The most common stationary energy storage devices are batteries and supercapacitors: in this research activity, the authors propose the same model regardless of whether it is a battery or a supercapacitor (Figure 10). The proposed energy storage device model is composed of the following elementary

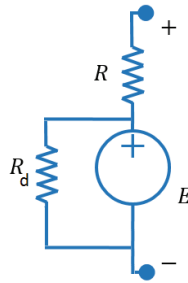


Figure 10: Scheme of the battery and supercapacitor model.

elements:

- An ideal voltage generator E (for the supercapacitor, the voltage is proportional to the integral of the current, while for the battery, the voltage is a non-linear function of the integral of the current);
- A resistance R_d in parallel with the voltage source which simulates the device transient discharge;
- A resistance R in series with the previous two elements.

This quite a simple modelling approach that allows the behaviour of batteries and supercapacitors, to be correctly simulated while requiring only a reduced set of parameters to work. Furthermore, this energy storage device, as a result of the modularity of the Simscape approach, can be easily connected in parallel with the electrical substations, allowing to simulate different scenarios and to search for the optimal spatial

distribution of energy storage devices throughout the line: in fact, for each specific application, it is possible to find the optimal distance between each stationary storage device in order to maximize the energy recovery and minimize the losses due the impedance of the line itself. In this research work, the authors mainly discuss the possibility of applying energy storage devices along the line, in particular connected in parallel to power substations used to feed the catenary; hence, the preliminary results shown in the paper are mainly referred to this system configuration. However, the application of the proposed model can be easily extended to the analysis of different solutions involving the use of energy storage systems to improve efficiency of regenerative braking. In particular, it is also possible to investigate different layouts in which energy storage devices are located on-board the vehicle. A large number of different energy storage scenarios can be investigated with the proposed model; however, in this phase of the research activity, the attention of the authors has been focused on the calibration and validation of the approach and on the preliminary analysis of the influence of stationary storage systems connected in correspondence of the electric substations.



Figure 11: Test case for the validation.

6 Validation and results

The proposed model has been tested and experimentally calibrated and validated considering the characteristics of a new Italian high speed train, the ETR 1000; the characteristics of the train, which must be considered in the proposed model, are given in Figures 7 and 11 and in Table 2. The approach has been used to simulate various different scenarios, all of them simulated on the same line (representative of the Firenze-Roma line, as reported in Figure 12, where the position of the electrical substations and the slope of the line are shown).

Train mass	495 t
Motorized weight fraction	0.5
Nominal power	9.8 MW
Nominal speed	300 km/h
Brake pad 1	0.1-0.15 cm ³ /MJ
Brake pad 2	0.1-0.21 cm ³ /MJ
Line impedance	0.05 Ω/km
ESS equivalent impedance	0.1 Ω
ESS no-load voltage	3700 V
Mean distance between ESSs	14.7 km
Max. distance between ESSs	76 km
Min. distance between ESSs	12 km

Table 2: Train and line characteristics.

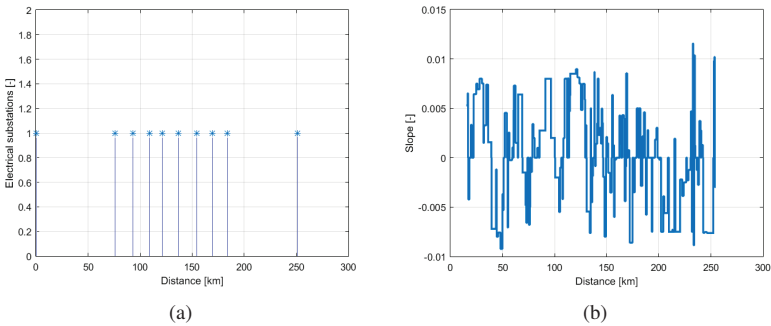


Figure 12: Scheme of the considered line: (a) substations and (b) slope.

Figure 13 shows the results referred to a preliminary analysis, performed considering a simple mission profile (*i.e.* a first acceleration, an 83 m/s constant speed period and a final braking) through the complete line in order to understand the global behaviour of the model. First of all, Figure 13(a) shows the velocity profile, calculated with the proposed model: it is in good agreement with the chosen mission profile. The results, shown in Figure 13, correspond to that velocity profile: it is possible to highlight how the higher power values corresponds to the initial acceleration phase up to the maximum speed (Figure 13(b), analogously to the higher absorbed current (Figure 13(c) and to the bigger voltage drop (Figure 13(d)). The other peaks and drops correspond to electrical substations and smaller accelerations due to the line characteristics; during the braking phases the voltage does not rise over the substation value because those results are referred to an operating scenario without energy recovery.

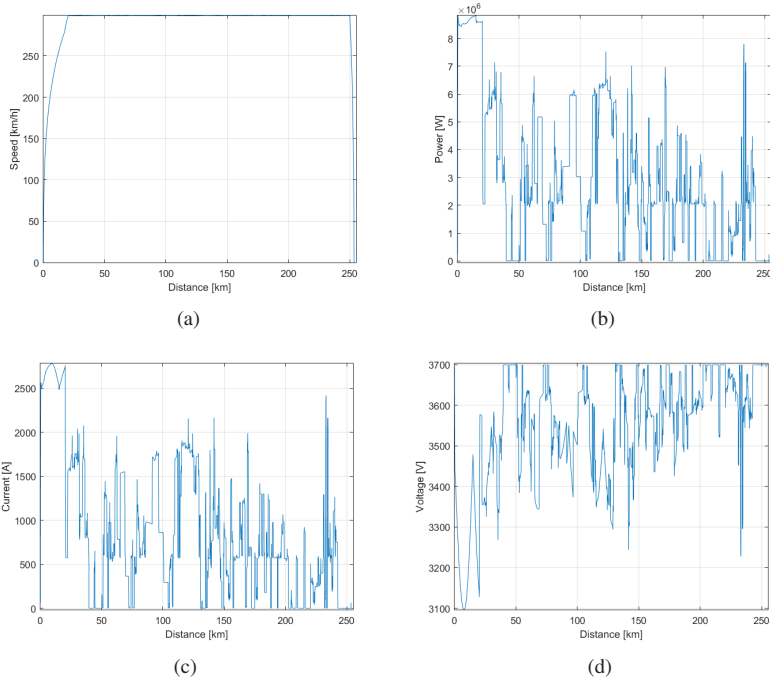


Figure 13: Preliminary results: (a) vehicle velocity profile, (b) power, (c) current and (d) voltage.

6.1 Model experimental calibration

The proposed model has been calibrated using a first set of experimental measurements referred to a traction manoeuvre of the ETR 1000 high speed train on a brief part of the Firenze-Roma line, from standstill to 250 km/h. The data are referred to an operating scenario where the applied traction effort is maximum (according to the performance data shown in Figure 7). Figure 14 shows the comparison between the results obtained with the proposed model and the experimental measurements. Figure 14(a) shows the mission profile imposed to the vehicle to simulate the experimental case. Figures 14(b) Figure 14(c) and Figure 14(d) show respectively the power, the absorbed current and the voltage in correspondence of the vehicle pantograph. It is possible to highlight how the power increases up to the iso-power part of the vehicle traction characteristic (*i.e.* the velocity rises for the entire simulation) and how the current and the voltage show respectively a drop and a peak in correspondence of a substation placed in the line segment considered. Furthermore, the test and the simulation begin when the vehicle is stationary: in these initial conditions, the only power consumption is represented by that required to feed the train auxiliary systems (*e.g.*

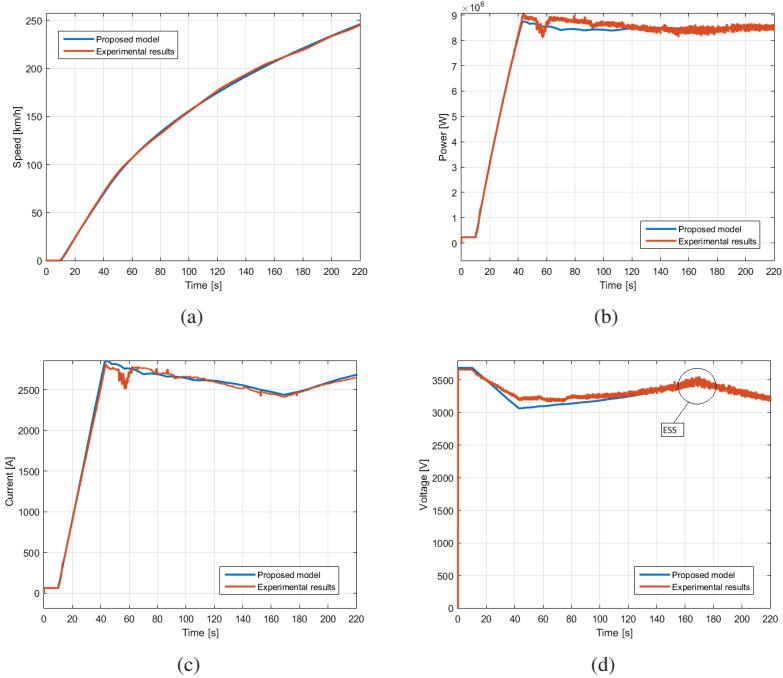


Figure 14: Model calibration: (a) vehicle velocity profile, (b) power, (c) current and (d) voltage.

air conditioning), which is equal to about 230 kW.

The results shown in Figure 14, being referred to a quite short part of the line, have allowed the authors to better calibrate the results provided by the proposed model by evaluating the technical data of the system affected by the greatest uncertainties. Figure 14(a) (*i.e.* the comparison between the experimental and simulated velocity profile) shows how the principal parameters concerning the traction system, the train inertia and the motion resistance were correct. The error in terms of speed profile is not completely negligible only between 80 and 120 km/h: in this operating range in fact the adhesion conditions during the experimental tests caused the onset of the axle skidding phenomenon. The implementation within the proposed model of an anti-skidding system could allow to improve the agreement with the experimental data even in presence of particular adhesion conditions.

An important parameter, which have been carefully evaluated in this calibration phase, is the train global efficiency η_{tot} , which can be defined as follows:

$$\eta_{tot}(T_t, \dot{x}) = \eta_e \eta_m \begin{cases} W_m \geq 0 \Rightarrow \eta_{tot} = \frac{W_m}{W_e} \\ W_m < 0 \Rightarrow \eta_{tot} = \frac{W_e}{W_m} \end{cases} \quad (8)$$

Speed Range	Global efficiency η_{tot} at 100% of the traction effort
0-36 [km/h]	From 0.8 to 0.82
36-54 [km/h]	0.82
54-126 [km/h]	From 0.82 to 0.86
126-162 [km/h]	0.86
162-180 [km/h]	From 0.85 to 0.86
180-236 [km/h]	0.85
236-350 [km/h]	From 0.83 to 0.85

Table 3: Preliminary calculation of the global efficiency η_{tot} with 100% of the traction effort applied.

η_{tot} typically depends on the traction effort and on the vehicle speed; being the product of the mechanical (η_m) and electrical efficiency (η_e) of the transmission and traction system, it depends on the mechanical power W_m and on the corresponding electrical power W_e (either absorbed during the traction phases or regenerated during the braking phases).

Through the comparison between the simulated and measured power W_c it is possible to estimate the value of the train efficiency; in the proposed model η_{tot} is assumed to be a function of the vehicle speed, without taking into account the influence of the traction effort. However, this simplifying hypothesis could be acceptable since the mechanical efficiency shows an increasing trend as the power increases, while the electrical efficiency (due to power electronics components) is higher with lower collected powers, providing a mutual compensation. The value of the efficiency found in this calibration phase is about 0.84 (see Table 3): it should be noted that in the operating range between 80 and 120 km/h the efficiency is lower due to the axle skidding phenomenon.

The considered set of experimental data enables the evaluation of the main parameters of the electrical substations; in particular, the authors performed an analysis in order to improve the estimation of the ESSs no-load voltage and of the equivalent impedance. The no-load voltage V_0 can be estimated through the pantograph voltage value in correspondence of the initial stationary phase. In this standstill operating condition, the pantograph power is small and produces small losses, allowing the approximation to consider V_0 equal to the pantograph voltage V_c itself (see Figure 14(d)). Furthermore, when the train passes under the intermediate ESS, it is operating in an iso-power condition (see Figure 14(b) and the ESS produces a peak in the pantograph voltage profile; in this condition almost all the power required by the train is due to the considered ESS. Hence, the line circuit representation can be simplified, allowing the estimation of the ESS equivalent impedance R_0 :

$$V_c = V_0 - R_0 I_c \Rightarrow R_0 = \frac{(V_0 - V_c)}{I_c} \quad (9)$$

Finally, the analysis of the pantograph voltage and current (Figures 14(c) and 14(d)) enables better estimates of the line equivalent resistivity ρ .

6.2 Model experimental validation

After the calibration phase, the authors used two further sets of experimental measurements (referred to different line sections) to perform a validation of the model. The two sets are referred to mixed mission profiles: the first set (shown in Figure 15) includes two traction phases with an intermediate partial braking, while the second (shown in Figure 16) is composed of a traction phase followed by a full braking. The comparisons between experimental and simulated results concern the speed profile, the power consumption, the collected current and voltage; the model has been set up with the parameters previously tuned in the calibration phase. It is possible

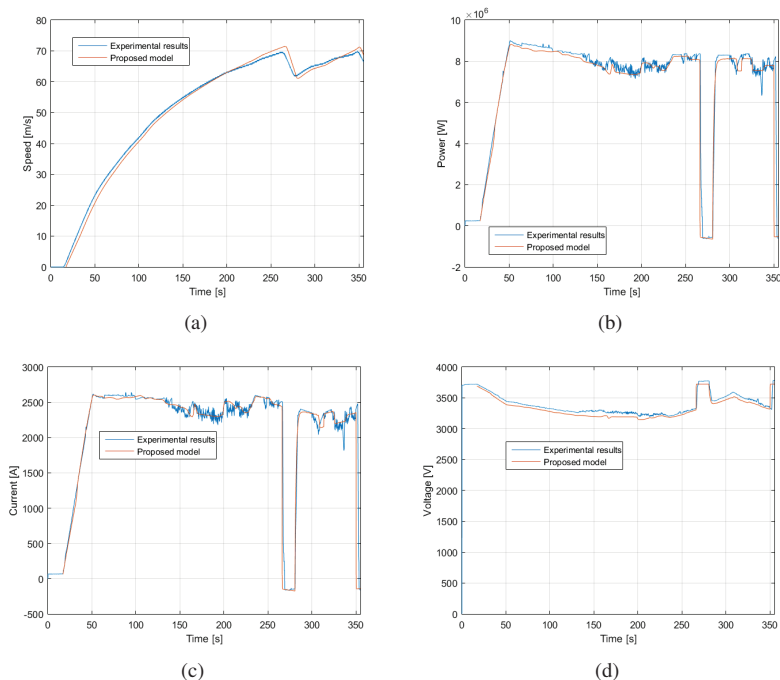


Figure 15: Experimental validation, first manoeuvre: (a) vehicle velocity profile, (b) power, (c) current and (d) voltage.

to highlight how the agreement between experimental and numerical results is quite good: the speed profile is well matched in both data sets, and also the power and current trends are quite well represented. The second part of the second manoeuvre

(i.e. the braking phase) is affected by greater errors, especially for the voltage profile: this can be partially due to degraded adherence conditions of the line. Furthermore, Figure 16 shows results which are referred to a line with non-reversible substations and without any other train/load that can support regenerative braking from the test vehicle (i.e. experimental activities are performed at night when commercial traffic is interrupted). In these conditions, since the equivalent load represented by the line is almost negligible, the response is highly influenced by second order phenomena (residual capacities, dispersion and loads of the line) which are not included in the proposed model since they are beyond the scope of the current research work. These phenomena are responsible for the high-frequency errors between the measured and simulated results during the braking phase. However, even in these conditions, the proposed model is able to properly represent the mean low frequency behaviour of the system. Furthermore, in presence of a line able to fully support regenerative braking, these effects provide negligible contributions to the behaviour of the system.

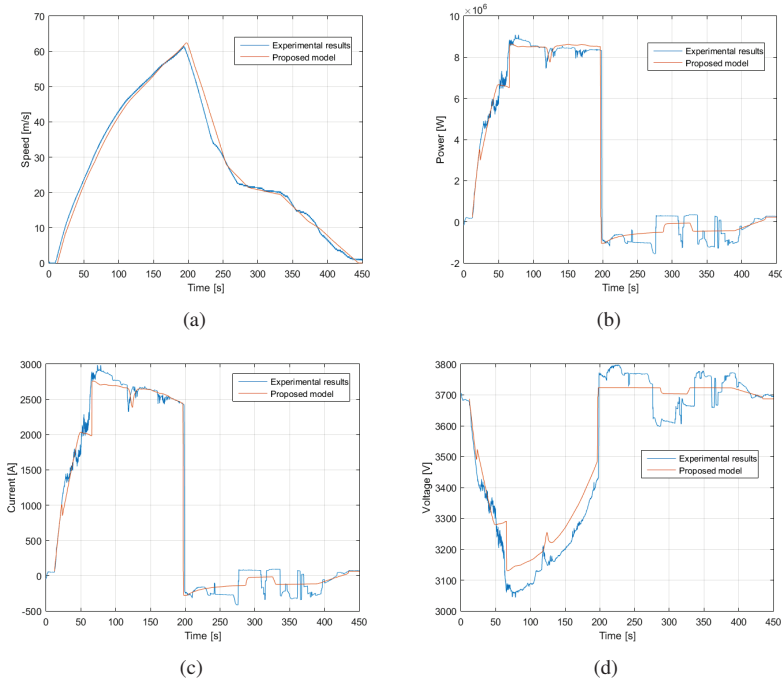


Figure 16: Experimental validation, second manoeuvre: (a) vehicle velocity profile, (b) power, (c) current and (d) voltage.

6.3 Energy considerations

After the calibration and the validation phases, the proposed model has been used to analyze the application of energy storage systems in high speed railways. This feasibility analysis has been performed considering the ETR 1000 and the “Direttissima” line; the mission profile used in the simulation is composed of an initial acceleration up to 70 m/s with the maximum traction effort, a constant speed phase and a final braking, applied considering different values of the requested braking effort. The final braking can produce a peak power of about 5 MW. The results, shown in this Section, are referred to the use of stationary energy storage devices. The authors have considered, concerning the validation and the feasibility analysis, only the braking phase: coasting ([43, 44]), and other optimization strategy based on the railway traffic, will be object of future investigation.

Figure 17(a) shows the terms which contribute to the braking energy calculated considering different values of the requested braking effort, which can be defined as follows:

$$\text{Braking request} = \frac{T_{b,des}}{T_{b,nom}} \quad (10)$$

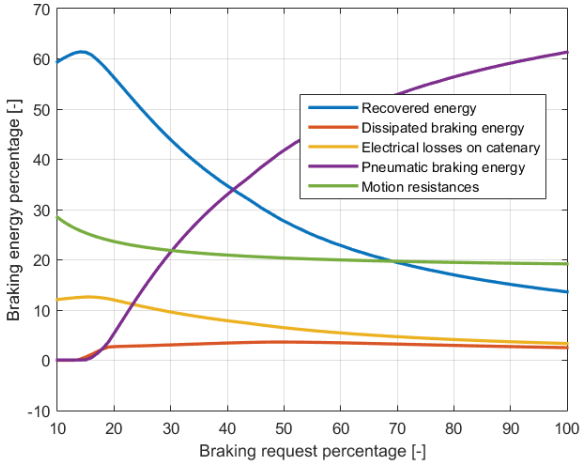
where $T_{B,nom}$ is the nominal braking effort calculated according to Figure 7. The braking request has a significant influence on the recovered energy: a higher braking request could reach the saturation of the braking effort and hence limit also the recovered energy; as shown in Figure 17(a), the braking energy, which can be recovered decreases as the request braking effort increases: this effect produces also an increment of the pneumatic braking energy.

Even with the simple mission profile considered in this analysis (*i.e.* single final braking), the electrical braking gives an important contribute in the energy balance. The regenerated energy has a maximum with a braking request lower than 20%, but this low value of the braking effort causes an unacceptable increase of the braking distance (shown in Figure 17(b) as a function of the braking request). A good compromise between recovered energy and braking distance can be found with a braking request of about 50%: in this operating condition it is possible to recover about 30% of the braking energy while maintaining the braking distance within acceptable limits.

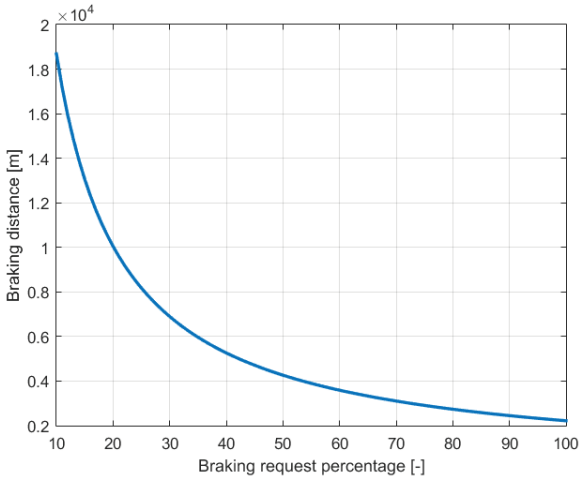
The energy dissipated on on-board resistors is due to a voltage limiter system implemented in the proposed model: if during the braking phase the pantograph voltage exceeds a safety limit (about 3900 V), regenerative braking is deactivated and the electrical braking becomes completely dissipative.

Furthermore, it is possible to highlight how the dissipated energy, due to mechanical losses, is lower when the braking effort is higher (*i.e.* when the braking distance is lower).

Figure 18 shows the voltage peak in correspondence of the regenerative braking phase, considering different braking effort requests and different braking starting points between two adjacent electric substations; the braking starting point can be



(a)



(b)

Figure 17: Energy flows involved in the braking phase (from 83 m/s to 0 m/s) (a) and braking distance with different braking efforts (b).

defined as follows (see Figure 6):

$$Braking\ position = \frac{x}{L_{12}} \tag{11}$$

The voltage peak initially increases with a steep slope (as a function of the braking

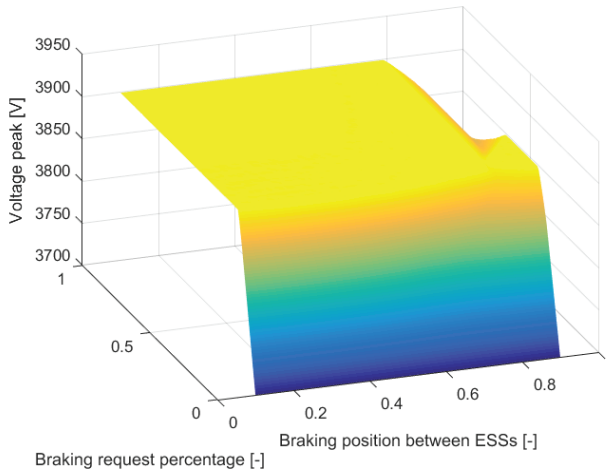


Figure 18: Braking voltage peak.

effort); after about 20% of the braking request the values are saturated by the voltage limiter (at 3900 V). The voltage values are always below the limit only near the electrical substations: if the braking phase begins near the ESS in fact the stationary storage device is able to manage all the energy flux provided by the vehicle.

7 Conclusions

In this paper the authors presented a tool able to simulate and to analyze different aspects of the railway vehicle dynamics. With respect to previous works presented in literature, the tool is designed to integrate different modules able to simulate various physical phenomena (*e.g.* electrical and mechanical), which influence the energetic behaviour and efficiency aspects of the railway system: the model is able to analyze the interactions between the vehicle longitudinal dynamics, the electrical behaviour of the contact line (including electrical substations) and the behaviour of stationary energy storage devices.

The proposed model has been developed and validated considering a benchmark case similar to a typical modern high speed train (*e.g.* the ETR 1000). The results of this analysis highlight two important aspects:

- from a modelling point of view, the proposed tool proved to be able to accurately reproduce the railway energetic aspects;
- from a physical point of view, the model highlights how energy storage systems can be useful even in high speed applications (*i.e.* applications where there is a

small number of braking phases), in order to save energy and thus increase the sustainability of the railway system.

In particular, a simple stationary solution can be really effective in high speed trains, while in tramways applications the use of on-board energy storage devices could be more worthy. In fact, for a high speed train the disadvantages due to an on-board energy storage device would be higher, especially considering the weight of the device and the small number of braking phases, while a stationary solution makes it easier to store the big but infrequent energy flows produced in the vehicle braking phase. Nowadays, those results are widely acknowledged even by other research works by professional operators of the sector. In a short time, a more accurate investigation including the introduction of a more sophisticated management of energy storage systems through power converters and the simulation of more complex scenario with multiple convoys traveling on the same line will be realized; it will be also possible to develop more realistic storage systems models. All these steps will require further validations through appropriate experimental data.

References

- [1] EU Transport Pocketbook 2013.
- [2] W.A. Kamal, "Improving energy efficiency - The cost-effective way to mitigate global warming", *Energy Conversion and Management*, 38(1), 39-59, 1997.
- [3] E. Fridell, A. Björk, M. Ferm, A. Ekberg, "On-board measurements of particulate matter emissions from a passenger train", *Proceedings of the Institution of Mechanical Engineers, Part F: Journal of Rail and Rapid Transit*, 225(1), 99-106, 2011.
- [4] M. Thiounn-Guermeur, "Evaluation of the hybrid locomotive PLATHEEA Platform for Energy Efficiency and Environmentally Friendly Hybrid Trains", *Proceeding of WCRR (World Congress of Railway Research)*, France, 2011.
- [5] S. Abbasi, A. Jansson, L. Olander, U. Olofsson, U. Sellgren, "A pin-on-disc study of the rate of airborne wear particle emissions from railway braking materials", *Wear*, 284, 18-29, 2012.
- [6] R. Gehrig, M. Hill, P. Lienemann, C.N. Zwicky, N. Bukowiecki, E. Weingartner, U. Baltensperger, B. Buchmann, "Contribution of railway traffic to local PM10 concentrations in Switzerland", *Atmospheric Environment*, 41(5), 923-933, 2007.
- [7] I. Salma, T. Weidinger, W. Maenhaut, "Time-resolved mass concentration, composition and sources of aerosol particles in a metropolitan underground railway station", *Atmospheric Environment*, 41(37), 8391-8405, 2007.
- [8] W.W. Marr, W.J. Walsh, P.C. Symons, "Modeling battery performance in electric vehicle applications", *Energy Conversion and Management*, 33(9), 843-847, 1992.

- [9] S. Hillmansen, C. Roberts, "Energy storage devices in hybrid railway vehicles: A kinematic analysis", *Proceedings of the Institution of Mechanical Engineers, Part F: Journal of Rail and Rapid Transit*, 221, 135-143, 2007.
- [10] D.K. Ware, R.N.H. Jones, "Recent developments in light rail systems", *Proceedings of the Institution of Mechanical Engineers, Part F: Journal of Rail and Rapid Transit*, 206(1), 47-65, 1992.
- [11] M.C. Falvo, et al., "Energy savings in metro-transit systems: A comparison between operational Italian and Spanish lines", *Proceedings of the Institution of Mechanical Engineers, Part F: Journal of Rail and Rapid Transit*, 230(2), 345-359, 2016.
- [12] A. Gonzalez-Gil, R. Palacin, P. Batty, "Optimal energy management of urban rail systems: Key performance indicators", *Energy Conversion and Management*, 90, 282-291, 2015.
- [13] R. Barrero, X. Tackoen, J. Van Mierlo, "Stationary or onboard energy storage systems for energy consumption reduction in a metro network", *Proceedings of the Institution of Mechanical Engineers, Part F: Journal of Rail and Rapid Transit*, 224, 207-225, 2010.
- [14] R. Teymourfar, B. Asaei, H. Iman-Eini, R. Nejati Fard, "Stationary supercapacitor energy storage system to save regenerative braking energy in a metro line", *Energy Conversion and Management*, 56, 206-214, 2012.
- [15] M. Ceraolo, G. Lutzemberger, "Stationary and on-board storage systems to enhance energy and cost efficiency of tramways", *Journal of Power Sources*, 264, 128-139, 2014.
- [16] A. Gonzalez-Gil, R. Palacin, P. Batty, "Sustainable urban rail systems: Strategies and technologies for optimal management of regenerative braking energy", *Energy Conversion and Management*, 75, 374-388, 2013.
- [17] A. Gonzalez-Gil, R. Palacin, P. Batty, J.P. Powell, "A systems approach to reduce urban rail energy Consumption", *Energy Conversion and Management*, 80, 509-524, 2014.
- [18] R. Barrero, J. Van Mierlo, X. Tackoen, "Energy savings in public transport", *Vehicular Technology Magazine, IEEE*, 3(3), 26-36, 2008.
- [19] M. Steiner, M. Klohr, S. Pagiela, "Energy storage system with ultracaps on board of railway vehicles", *Power Electronics and Applications, European Conference*, 1-10, 2007.
- [20] R. Conti, E. Galardi, E. Meli, D. Nocciolini, L. Pugi, A. Rindi, "Energy and wear optimisation of train longitudinal dynamics and of traction and braking systems", *Vehicle System Dynamics*, 53(5), 651-671, 2015.
- [21] E. Galardi, E. Meli, D. Nocciolini, L. Pugi, A. Rindi, "Development of efficient models of Magnetic Braking Systems of railway vehicles", *International Journal of Rail Transportation*, 3(2), 97-118, 2015.
- [22] L. Pugi, A. Rindi, A.G. Ercole, A. Palazzolo, J. Auciello, D. Fioravanti, M. Ignesti, "Preliminary studies concerning the application of different braking arrangements on Italian freight trains", *Vehicle System Dynamics*, 49(8), 1339-1365, 2011.

- [23] L. Pugi, M. Malvezzi, S. Papini, G. Vettori, “Design and preliminary validation of a tool for the simulation of train braking performance”, *Journal of Modern Transportation*, 21, 247-257, 2013.
- [24] L. Pugi, A. Palazzolo, D. Fioravanti, “Simulation of railway brake plants: An application to SAADKMS freight wagons”, *Proceedings of the Institution of Mechanical Engineers, Part F: Journal of Rail and Rapid Transit*, 222(4), 321-329, 2008.
- [25] A. Frilli, E. Meli, D. Nocciolini, L. Pugi, A. Rindi, M. Ceraolo, G. Lutzemberger, “Improved Sustainability of Railway Systems: The Tesys Rail Project”, in J. Pombo, (Editor), “*Proceedings of the Third International Conference on Railway Technology: Research, Development and Maintenance*”, Civil-Comp Press, Stirlingshire, UK, Paper 289, 2016. doi:10.4203/ccp.110.289
- [26] Official Web Site of E.R.A. <http://www.era.europa.eu>.
- [27] Regulation 1302/2014 (1st merged RST TSI) Eif/DoA: 1/1/2015.
- [28] Regulation 1301/2014 (1st merged ENE TSI) Eif/DoA: 1/1/2015 gulation 1301/2014 (1st merged ENE TSI) Eif/DoA: 1/1/2015.
- [29] Regulation 321/2013 (2nd CR WAG TSI) Eif 13/4/2013 DoA: 1/1/2014.
- [30] UIC Fiche UIC 544-1 Brakes-Braking Power, 6th edition, October 2014.
- [31] UIC Fiche UIC 541-3, Brakes - Disc brakes and their application - General conditions for the approval of brake pads Leaflet details 7th edition, October 2010 - Translation.
- [32] EN 15734-1 Railway applications - Braking systems of high speed trains Part 1: Requirements and definitions.
- [33] P.C. Breedveld, R.C. Rosenberg, T. Zhou, “Bibliography of bond graph theory and application”, *Journal of the Franklin Institute*, 328(5), 1067-1109, 1991.
- [34] E. Widl, P. Palensky, A. Elsheikh, “Evaluation of two approaches for simulating cyber-physical energy systems”, In *IECON 2012-38th Annual Conference on IEEE Industrial Electronics Society*, 3582-3587. IEEE, 2012.
- [35] L. Pugi, R. Conti, D. Nocciolini, E. Galardi, A. Rindi, S. Rossin, “A Tool for the Simulation of Turbo-Machine Auxiliary Lubrication Plants”, *International Journal of Fluid Power*, 15(2), 87-100, 2014.
- [36] L. Pugi, E. Galardi, C. Carcasci, A. Rindi, N. Lucchesi, “Preliminary design and validation of a Real Time model for hardware in the loop testing of bypass valve actuation system”, *Energy Conversion and Management*, 92, 366-384, 2015.
- [37] S. Baccari, G. Cammeo, C. Dufour, L. Iannelli, V. Mungiguerra, M. Porzio, G. Reale, F. Vasca, “Real-Time Hardware-in-the-Loop in Railway: Simulations for Testing Control Software of Electromechanical Train Components, Railway Safety, Reliability, and Security”, *Technologies and Systems Engineering*, 221-248, 2012.
- [38] M. Peña-Alcaraz, et al., “Optimal underground timetable design based on power flow for maximizing the use of regenerative-braking energy”, *Proceedings of the Institution of Mechanical Engineers, Part F: Journal of Rail and Rapid Transit*, 226(4), 397-408, 2012.
- [39] M. Ceraolo, G. Lutzemberger, T. Huria, “Experimentally-determined models for

- high-power lithium batteries”, *Advanced Battery Technology*, 2011.
- [40] E. Quaglietta, V. Punzo, “Supporting the design of railway systems by means of a Sobol variance-based sensitivity analysis”, *Transportation Research Part C: Emerging Technologies*, 34, 38-54, 2013.
- [41] L. Pugi, M. Malvezzi, R. Conti, ”Optimization of Traction and Braking Subsystems with respect to Mission Profile”, in J. Pombo, (Editor), ”Proceedings of the Second International Conference on Railway Technology: Research, Development and Maintenance”, Civil-Comp Press, Stirlingshire, UK, Paper 247, 2014. doi:10.4203/ccp.104.247
- [42] P. D’Adamio, J. Escalona, E. Galardi, E. Meli, L. Pugi, A. Rindi, ”Real Time Modelling of a Railway Multibody Vehicle: Application and Validation on a Scaled Railway Vehicle”, in J. Pombo, (Editor), ”Proceedings of the Third International Conference on Railway Technology: Research, Development and Maintenance”, Civil-Comp Press, Stirlingshire, UK, Paper 259, 2016. doi:10.4203/ccp.110.259
- [43] K. Kim, S. Chien, “Simulation-based analysis of train controls under various track alignments”, *Journal of Transportation Engineering*, 136(11), 937-948,2010.
- [44] L. Allen, S. Chien,“Reducing Rail Energy Consumption through Coasting and Regenerative Braking“, *Proceedings of the Transportation Research Board 96th Annual Meeting*, 2017.

Nomenclature

F_a	Rolling resistance term
F_c	Curves and line design contribution term
F_i	Inertial term
F_p	Slope contribution term
F_t	Longitudinal traction and braking efforts
L_{12}	Distance between two consecutive substations
R	Resistance
R_0	ESS equivalent impedance
T	Effort
V	Voltage
W	Power
W_r	Recovered braking power
a	Vehicle motion resistance coefficient
b	Vehicle motion resistance coefficient
c	Vehicle motion resistance coefficient
f_b	Braking frequency
g	Gravity acceleration
i	Current

p_c	Curves resistance coefficient
m	Mass
m_i	Train inertia
x	Vehicle position
\dot{x}	Vehicle speed
\ddot{x}	Vehicle acceleration
v	Velocity

Greek Letters

α	Line slope
δ	Adimensional vehicle position
η	Efficiency

Subscripts and Superscripts

0	No-load
b	Braking
c	Pantograph
dc	Ideal voltage source
des	Desidered
e	Electrical
$gearbox$	Transmission system
$left$	Left
m	Mechanical
max	Maximum
$mean$	Mean
$motor$	Electric motor
$motordrive$	Motor drive
n	n -th node
nom	Nominal
$right$	Right
sub	Substation
t	Traction
tot	Total
v	Required or provided
$wheels$	Wheel/rail contact point